Slov Vet Res 2019: 56 (2): 59–74
DOI 10.26873/SVR-610-2019
UDC 616.16-006:615.277.3:582.282.123.4

Original Research Article

PSEUROTIN A FROM *Aspergillus fumigatus* Fr. AUMC 8002 EXHIBITS ANTICANCER ACTIVITY AGAINST HEPATOCELLULAR CARCINOMA *IN VITRO* AND *IN VIVO*

Gamal A. Helal[1], Fatma A. Ahmed[2], Ahmed Askora[1], Taghred M. Saber[3]*, Shimaa M. Rady[1,2]

[1]Department of Microbiology and Botany, Faculty of Science, Zagazig University, Zagazig 44519, [2]Medicinal and Aromatic Plants Department, Desert Research Center, El-Mataria, Cairo, [3]Forensic Medicine and Toxicology Department, Faculty of Veterinary Medicine, Zagazig University, Zagazig 44519, Egypt

*Corresponding author, E-mail: taghredsaber1982@gmail.com

Abstract: This study investigated the *in vitro* and *in vivo* anti-hepatocellular carcinoma activity of pseurotin A isolated from the n-butanol extract of *Aspergillus fumigatus* Fr. AUMC 8002 (nBE-AF).The *in vitro* anticancer activity of nBE-AF was measured against a human hepatocellular carcinoma cell line (HepG2) using a sulforhodamine-B (SRB) assay. The intraperitoneal median lethal dose (LD_{50}) of nBE-AF was determined in rats. Hepatocellular carcinoma was induced in rats by a single intraperitoneal injection of diethylnitrosamine (DEN) (200 mg/kg b.wt.) followed by subcutaneous injections of carbon tetrachloride (CCl_4) (3 ml/kgb.wt.) weekly for 6 weeks. After administration of these carcinogens, 1/10 and 1/20 LD_{50} doses of nBE-AF were administered intraperitoneally daily. NBE-AF exhibited significant cytotoxic activity against HepG2 cells. Administration of DEN and CCl_4 significantly elevated the serum levels of liver function and tumour markers and significantly downregulated tumour necrosis factor-α gene expression. Moreover, DEN and CCl4 decreased immunohistochemical Bax expression and increased Bcl-2 expression in the liver. Co-treatment with nBE-AF mitigated the DEN+CCl_4-induced alterations in a dose-dependent manner. Histopathological evaluation of the liver substantiated the above biochemical results. These results confirmed that nBE-AF, via its major isolated secondary metabolite, pseurotin A, exerted an anti-hepatocarcinogenic effect and could be used as a chemopreventive agent for hepatocellular carcinoma..

Key words: *Aspergillus fumigatus* extract; pseurotin A; hepatocellular carcinoma; anticancer; cytotoxic

Introduction

Cancer is a leading cause of death worldwide. Approximately 7.6 million deaths occur from cancer annually worldwide, and this number is expected to increase to 13.1 million in 2030 (1). Hepatocellular carcinoma (HCC) is the fifth most common tumour and the second most common cause of cancer mortality worldwide (2). The major risk factors for HCC are hepatitis B or C virus infection, food additives, toxic industrial chemicals, alcohol consumption, and exposure to environmental carcinogens such as aflatoxins and nitrosamines (3). Diethylnitrosamine (DEN) is one of the most potent hepatocarcinogenic nitrosamines found in agricultural chemicals, cosmetics and alcoholic beverages (4). DEN has been commonly used as a cancer initiator for the induction of HCC in experimental animals. Metabolized DEN in the liver generates reactive oxygen species (ROS) and induces oxidative stress and liver cell injury (5, 6).Furthermore, DEN is a genotoxic compound that forms alkyl DNA adducts and causes several nuclear aberrations in the rat liver that ultimately lead to the development of HCC (7).Carbon

Received: 12 August 2018
Accepted for publication: 12 April 2019

tetrachloride (CCl_4) is a powerful environmental toxicant that produces severe hepatic damage via the generation of reactive free radicals. Currently, there is no established effective chemotherapy for liver cancer, and chemotherapy is considered of limited value (8).One current approach to control hepatic cancer is chemoprevention, a programme of cancer management in which the occurrence of tumourigenesis could be completely prevented, slowed, or reversed by the use of natural or synthetic products (9).Indeed, the complementary and alternative use of natural products in the treatment of liver diseases has greatly increased worldwide. Currently, the identification of bioactive ingredients from plants, marine organisms and microorganisms to inhibit tumourigenesis in different types of animal models of carcinogenesis is attracting substantial attention (10). Fungi are important sources of bioactive secondary metabolites containing novel compounds with unique structural characteristics. These organisms have proven to be a rich and promising source of novel anticancer, antibacterial, antitumour and anti-inflammatory agents (11). *Aspergillus fumigatus* is a saprotrophic fungus that is widespread throughout nature. *A. Fumigatus* is found in soil and decaying organic matter and plays a vital role in carbon and nitrogen recycling. Numerous bioactive compounds, such as alkaloids, dibenzofurans, dioxopiperazine and indolediketopiperazine, have been isolated from *A. fumigatus* (12, 13). In the present study, subsequent culture and fractionation of the n-butanol extract of *A. fumigatus* (nBE-AF) resulted in the isolation of pseurotin A as a major secondary metabolite. Pseurotin A (an alkaloid) is a major secondary metabolite isolated from *Pseudeurotium ovalis* (14) and *A. Fumigatus* (15).To our knowledge, detailed studies about the anticancer effects of pseurotin A have not yet been reported. Therefore, the aim of this study was to evaluate the chemopreventive effect of nBE-AF via its major isolated secondary metabolite, pseurotin A, against HCC in rats.

Materials and methods

Chemicals

DEN was purchased from Sigma Chemicals Co. (St. Louis, MO, USA), whereas CCl_4 was obtained from El-Gomhoria Chemicals Co. (Zagazig, Egypt).

Fungal strain and growth conditions

The *Aspergillus fumigatus* Fr. AUMC 8002 strain was previously isolated and characterized from Roquefort cheese from the Sharkia and Assiut Governorates, Egypt. This fungal strain was maintained on Czapek yeast extract agar medium and incubated at 30ºC for 7 days, followed by monthly subculture.

N-butanol extract of A. fumigatus Fr. AUMC 8002

An Erlenmeyer conical flask(250 ml capacity) containing 50 ml of Czapek yeast extract broth medium was inoculated with 1 ml of *A. fumigatus* Fr. AUMC 8002 fungal spore suspension, and the culture flasks were incubated at 30°C for 7 days. After incubation, the fermented substrate was extracted using 1:1(v/v) n-butanol. The n-butanol extracts were washed with equal volumes of distilled water and dried over anhydrous sodium sulfate, filtered and concentrated by air-drying. The obtained crystals were preserved in dark bottles in a refrigerator at 4ºC and subjected to further analysis.

In vitro anticancer activity

The *in vitro* anticancer activity of nBE-AF against HepG2 cells was measured using a SRB assay (16). Briefly, cells were placed in a 96-multiwell plate (104cells/well) for 24 h before treatment with the compounds to allow attachment of the cells to the surface of the plate. nBE-AF was dissolved in dimethylsulfoxide (DMSO), and different concentrations (5, 12.5, 25 and 50 mM) were added to the cell monolayer. Triplicate wells were prepared for each individual dose. The cell monolayer was incubated with nBE-AF for 48 h at 37°C in an atmosphere of 5% CO_2. After 48 h, cells were fixed, washed and stained for 30 min with 0.4% (w/v) SRB dissolved in 1% acetic acid. Unbound dye was then removed by four washes with 1% acetic acid, and the bound stain was recovered with Tris-EDTA buffer. The colour intensity was measured in an enzyme-linked immunosorbent assay (ELISA) reader (microplate reader; Sunosik; SPR-960B; China). The relationship between the surviving fraction and the nBE-AF concentration was plotted to obtain the survival curve for the

HCC cell line after the specified time, and the IC_{50} (the concentration required for 50% inhibition of cell viability) was calculated.

Isolation and chemical identification of the major compound isolated from nBE-AF

The extract was subjected to silica gel open column chromatography [Merck silica gel 60H (70–203 mesh)] and elution with a stepwise gradient of 100% hexane to 100% EtOAc to (1:1) EtOAc-MeOH to yield 4 major fractions (F1-F4).

Fraction (3), eluted with hexane–EtOAc (7:3), yielded a pale yellow solid precipitate, which was purified by recrystallization from MeOH to yield pseurotin A. Thin-layer chromatography (TLC) was carried out using Merck Kiesel gel 60 pf254 plates. Preparative TLC was used for purification of the compound using chloroform and methanol (4:1) as the mobile phase, yielding a white crystalline solid. The chemical structure of the isolated compound was elucidated according to elemental analysis of C, H, N and halogen in a Perkin Elmer CHN 2400 and spectroscopic analysis including infrared (IR), nuclear magnetic resonance (^{1}HNMR), carbon-13 nuclear magnetic resonance (^{13}C NMR) and mass spectra. These analyses were carried out at the Micro-analytic Center, Cairo University, Egypt, as follows:

IR spectra

The IR spectra of the isolated compound were recorded from KBr discs using an FTIR Spectrophotometer 460 (4000–400 cm^{-1}).

Mass spectra

The mass spectra (direct inlet, FAB ionization) of the isolated compound were recorded using a mass spectrophotometer (MS-5988). The product was subjected to a stream of high-energy electrons at elevated temperatures of up to 100°C, yielding cleavage fragments, which were characterized by the mass/charge (m/e) values from the mass spectral data.

^{1}HNMR

Spectra were recorded on a Varian Mercury VX-300 NMR spectrometer using DMSO-d6 as a solvent and tetramethylsilane (TMS) as the internal chemical shift reference. Shifts (in ppm relative to TMS, with coupling constants in Hz) were obtained with the Varian Mercury VX-300 NMR spectrophotometer (500 MHz for ^{1}H and 125 MHz for ^{13}C).

Animals

Healthy adult male Sprague-Dawley rats weighing 150–170 g were provided by the Animal Research Unit, Faculty of Veterinary Medicine, Zagazig University, Egypt. Animals were acclimated to laboratory conditions for 2 weeks prior to starting the experiment. Rats were kept in metal cages during the experimental period, maintained on a 12 h light-dark cycle in a temperature range of 21–24 °C and a relative humidity of 50–60%, and supplied a standard diet. The protocols were approved by the Ethics of Animal Use in Research Committee of Cairo University.

Determination of the intraperitoneal median lethal dose (LD_{50})

An acute toxicity screen was performed for nBE-AF according to the Spearman-Karber arithmetic method (17). Eighty-four adult male Sprague-Dawley rats were divided into 14 groups (six per group). The animals were fasted overnight with only water provided. The control group received no treatment. Groups 2 through 14 received intraperitoneal injections of fungal extract dissolved in water at different concentrations ranging from 500 to 6500 mg/kg body weight (b.wt.). The mortality of the animals was observed after 24 h.

$LD_{50} = LD100 - \sum (a \times b)/n$

n = total number of rats in a group.

a = difference between two consecutive doses of injected fungal extract.

b = average number of dead animals between two succeeding doses.

LD_{100} = lethal dose leading to 100% death of all test animals.

Induction of HCC

HCC was induced by a single intraperitoneal injection of DEN at a dose of 200 mg/kg b.wt.

dissolved in normal saline, as previously described by Sarkar et al. (18). After two weeks, animals received subcutaneous injections of CCl_4 in corn oil (50% (v/v), 3 ml/kg b.wt.) weekly for 6 weeks to promote the carcinogenic effect of DEN (6).

Experimental design

Sixty rats were divided into six groups (10/group) for an experimental period of 32 weeks. Group I served as the normal control group and received vehicle alone. Group II was the HCC (DEN+CCl_4) control rat group. Groups III (DEN+CCl_4+ 1/10 LD_{50}) and IV (DEN+CCl_4+ 1/20 LD_{50}) were injected intraperitoneally with fungal extract dissolved in distilled water at doses of 508 and 254 mg/kg b.wt., respectively, daily. Group V (1/10 LD_{50}) was intraperitoneally injected with 508mg/kg b.wt. nBE-AF alone daily. Group VI (1/20 LD_{50}) received intraperitoneal injection of nBE-AF alone (254 mg/kg b.wt.) daily. At the end of the experiment, blood samples were collected from the medial canthus of the rats and were centrifuged at 3000 rpm for 10 min to separate serum. Serum samples were preserved at -20°C until use for biochemical analysis. Then, rats were anaesthetized using diethyl ether and sacrificed by cervical dislocation, and liver tissue was rapidly removed and perfused with ice-cold saline. Liver specimens were immediately frozen in liquid nitrogen and stored at -80°C for analysis of gene expression. Other liver specimens from all groups were preserved at -20°C for the assessment of antioxidant status or in 10% neutral buffered formalin for histopathological and immunohistochemical investigations.

Biochemical analysis

Assessment of liver function

Serum activities of alanine aminotransferase (ALT) and aspartate aminotransferase (AST) were estimated according to the method described by Bergmeyer et al. (19). Serum alkaline phosphatase (ALP) activity was measured by the method of King and Armstrong (20).Serum levels of albumin, total protein and total bilirubin (TBL) were determined according to the methods described by Grant etal. (21) and Tietz (22, 23), as appropriate.

Quantitative determination of serum tumour markers

Alpha-fetoprotein (AFP) and carcinoembryonic antigen (CEA) levels were measured using ELISA kits provided from Bio-Check, Inc. (Foster City, CA, USA).

Assessment of antioxidant activity

Liver specimens were homogenized (10% (w/v)) in a potassium phosphate buffer solution (pH 7.4) using a tissue homogenizer. Samples were then centrifuged at 3000 rpm for 15 min. The supernatant was used to estimate superoxide dismutase (SOD) activity (24), catalase (CAT) activity (25), glutathione peroxidase (GPx) activity (26), reduced glutathione (GSH) levels (27) and malondialdehyde (MDA) concentrations (28).

Estimation of hepatic tumour necrosis factor-α (TNF-α) expression

Total RNA was extracted from 30 mg of liver tissue using an RNeasy Mini Kit (Qiagen, Heidelberg, Germany) according to the manufacturer's instructions. The purity of the total RNA was determined using a NanoDrop® ND-1000 spectrophotometer (NanoDrop Technologies, Wilmington, Delaware, USA). Total RNA (0.5 µg) was reverse transcribed into cDNA using a Qiagen LongRange2 Step RT-PCR Kit following the manufacturer's instructions. One microliter of total cDNA was mixed with 12.5 µl of 2× SYBR® Green PCR Mix with ROX from BioRad, 5.5 µl of autoclaved water, and 0.5 µl (10 pmol/µl) of each forward and reverse primer for the target genes. The expression values were normalized to an internal housekeeping control (*β*-actin) gene. The expression of the TNF-*α* gene was assessed using real-time PCR. The primer sequences are shown in Table (1). PCR reactions were conducted in a Rotor-Gene Q cycler (Qiagen, Heidelberg, Germany). The real-time qPCR program included an enzyme activation step at 94°C for 2 min followed by 40 cycles of denaturation at 95°C for 15 sec, annealing at 60 °C for 30 sec and extension at 72 °C for 30 sec. Detection of the fluorescent product was carried out at the end of the 72 °C extension period. The amplification data were collected by a sequence detector and analysed with sequence detection software. For each assay, a standard curve was generated using increasing amounts of cDNA, and the slopes of all curves indicated adequate PCR conditions (slopes of 3.3-3.6). The RNA concentration in each sample was determined from the threshold cycle (Ct) values and calculated with the sequence detection software supplied by the manufacturer. The quantitative fold changes

in mRNA expression were determined relative to the ß-actin mRNA levels in each corresponding group and calculated using the $2^{-\Delta\Delta Ct}$ method.

Histopathological examination

Liver samples were preserved in 10% neutral buffered formalin and were then processed and stained with haematoxylin and eosin (H&E) for histopathological examination using light microscopy (29).

Immunohistochemical investigation

Liver sections were prepared for immunohistochemical detection of Bax and Bcl-2 using primary rabbit polyclonal anti-rat Bax and Bcl-2 antibodies (Thermo Fisher Scientific Inc., Fremont, CA, USA), respectively. This technique was carried out via the avidin–biotin complex method (30). Negative control sections were incubated in phosphate-buffered saline instead of the primary antibody, and all tissue sections were examined under a light microscope.

Statistical analysis

The data are presented as the means ± standard error (SE). Statistical analysis was performed using one-way analysis of variance (ANOVA) followed by the post hoc Duncan's test for comparison between different experimental groups. Analyses were performed using IBM SPSS statistics computer software (version 22). P-values of < 0.05 were considered statistically significant.

Results

In vitro anticancer potency

To explore the *in vitro* anticancer potency of nBE-AF against HepG2 cells, cell proliferation was determined by an SRB assay. The cytotoxic effects of nBE-AF on HepG2 cells were determined by treating cells with different concentrations of nBE-AF. Upon treatment with increasing concentrations of nBE-AF, treated cells showed a significant decrease in viability. nBE-AF was active against HepG2 cells, with an IC_{50} of 22.2 µg/ml (Figure 1).

Preliminary characterization of nBE-AF

nBE-AF is a faint yellow-green colour and dissolves only in DMSO with heating and shaking and in hot water. nBE-AF produces one yellow spot on TLC with an R_f value of 0.3 using methanol solvent and melts at 203°C. Elemental analysis indicated that the ratio of the main elements (C/H/N) was 2.73/2.77/0.33 for compound 32. The extracted natural compound was found to be a polymer of the furanose ring with n=3 units. The data obtained by spectral analysis, IR spectrophotometry and mass spectrometry indicated that the M^+ parent ions were a polymer of the furanose ring. The mass spectrometry data showed that the M^+ parent ion (430) indicated n= 3 fragmentation, and the IR spectra showed the presence of bands at 1116 and 1039 cm-1, corresponding to the ether linkage (-O-) and (C=C), respectively, in the furanose moiety (Helal et al., 2018 unpublished data).

Chemical identification of the major compound isolated from nBE-AF

Preparative chromatographic purification of nBE-AF yielded the pseurotin A compound as the major compound isolated from nBE-AF. The molecular formula of this compound was determined using spectroscopic tools (IR, ^1H and ^{13}C NMR, elemental analysis and mass spectrometry) as illustrated in Figure 2. The structure of pseurotin contains a unique and highly oxidized azaspirocyclic framework in the form of a 1-oxa-7-azaspiro[4.4]non-2-ene-4,6-dione ring system. Numerous analogues were found that differed in the substitution at positions C2 and C8 (Figure 2).

IR (KBr, cm^{-1})

The IR spectra showed absorption bands for hydroxyls and NH groups: 3399 cm^{-1} (br, 3OH and NH), 3080 cm^{-1}(C-H, aromatic), 2936 cm^{-1} (C-H aliphatic), 1656 cm^{-1} (br, 3C=O, α, β-unsaturated and amidic), and 1246 cm^{-1} (-O-, ether).

^1H NMR (DMSO-d6)

The ^{1}HNMR data indicated shifts with δ= 2.52, 2.72, 2.88 and 2.52 ppm (t, J=3H, CH3, CH2); 2.72 and 2.88 (2s, J=6H, 2CH3); 3.05 (q, 2H, CH2CH3);

3.40, 3.53, and 3.79 (3t, 2CHOH); 3.87(s, 1H, NH, exchange with D2O); 4.26, 4.88, and 5.17 (3t, 3OH, exchange with D2O); 6.56 (d,1H, J= 10.2 Hz olefinic); 6.96 (d, 1H, J = 16.9 Hz, olefinic); and 7.89(s,5H, Ar-H).

13C NMR (DMSO-d6)

The ^{13}C NMR results indicated shifts with δ = 29.81, 31.29, 35.20, and 36.33 (3CH3 and CH2); 63.48, 70.07, 70.32 and 75.25 (4CHOH); 81.37, 92.17, 92.62, 97.26, 98.49, 102.3, 104.4, and 104.6 (2C=C and 4Ar-C); and 162.9, 174.2 and 179.8 (3C=O).

Mass spectrometry

The fast atom bombardment mass spectrometry (FABMS) data contained a peak (m/z= 432 [M+H]+), identified as C22H25NO8, that indicated the parent ion at M+1 [m/z= 431.45 (M + H+, 19.54%)] with fragment ions at m/z values of 54.95 (67.56%), 57.10 (72.88%), 69.10 (99.75%), 70.05 (61.02%), 71.10 (69.86%), 81.05 (67.17%), 83.05 (92.59%), 85.05 (73.24%), 97.10 (100%) as the base peak, 111.0 (63.06%), and 430.35 (47.96%).

The parent ion indicates that the molecular formula of this compound is $C_{22}H_{25}O_8N$; the compound was soluble in ethyl acetate, acetone, ethanol and isopropanol.

Median lethal dose of nBE-AF

The intraperitoneal LD_{50} of nBE-AF in rats was 5083 mg/kg b.wt., suggesting that nBE-AF was highly safe. The therapeutic doses were (1/10 of the LD_{50}) 508.3 mg/kg b.wt. and (1/20 of the LD_{50})254.2 mg/kg b.wt. (Table 2).

Effect of nBE-AF on liver function and serum tumour markers

DEN+ CCl_4-treated rats showed significantly ($p < 0.05$) increased serum ALT, AST and ALP activity and TBL levels compared with those of the control group. However, the groups co-treated with DEN and nBE-AF (III and IV) exhibited significant dose-dependent reduction in the levels of these markers compared with those in the DEN+CCl_4-treated group. In addition, the serum albumin and total protein levels were significantly decreased in rats treated with DEN and CCl_4 relative to those in control group. Compared with DEN+CCl_4 treatment alone, co-administration of nBE-AF with DEN significantly increased serum albumin and total protein (Table 3).The serum levels of the tumour markers AFP and CEA were significantly increased in the DEN+CCl_4-treated group compared with those in the control group but were significantly decreased by co-treatment with 1/10 and 1/20 LD_{50} doses of nBE-AF (Figure 3).

Effect of nBE-AF on hepatic antioxidant status

The activities of the hepatic antioxidant enzymes GR, GPx and SOD were significantly decreased in DEN-treated group compared with those in control animals (Table 4). Compared to the DEN-treated group, the groups treated with nBE-AF showed significantly increased hepatic GR, GPx and SOD activities (Table 4). A significant increase in the MDA level, which is a marker of lipid peroxidation, was observed in DEN-treated rats relative to that in control rats (Table 4). Treatment with nBE-AF for 24 weeks showed a significant protective effect against DEN-induced lipid peroxidation (Table 4). Therapeutic treatment with nBE-AF for 24 weeks resulted in a significant decrease in MDA levels compared to those in DEN-treated rats (Table 4). DEN administration led to a significant reduction in hepatic GSH content compared with that in control rats (Table 4), but treatment with nBE-AF significantly improved hepatic GSH levels compared to those in DEN-treated group (Table 4).

Estimation of hepatic TNF-a expression

Expression of the TNF-*a* gene was significantly ($p < 0.05$) upregulated in the livers of DEN+CCl_4-treated rats relative to that in control group rats. Additionally, this expression level was significantly downregulated in a dose-dependent manner in the nBE-AF-co-treated groups (III and IV) relative to that in theDEN+CCl_4-treated group (Figure 4).

Histopathological changes

Light microscopy of H&E-stained liver sections from rats in the control and nBE-AF-treated groups

showed normal polygonal hepatocytes with round nuclei arranged in strands, along with a normal central vein, Kupffer cells and blood sinusoids (Figure 5A). The livers of rats in the DEN+CCl_4-treated group revealed highly demarcated HCC near the central vein and some hepatocytes with a vacuolated cytoplasm and deeply stained pyknotic nuclei, in addition to dilated blood vessels (Figure 5B). Severely congested blood vessels and hepatic portal vein, along with portal vein dilation, were also observed (Figure 5C). The lesions in the group treated with DEN+CCl_4+1/10 LD_{50} nBE-AF were distinctly reduced relative to that in the DEN-treated group. The livers of rats treated with DEN+CCl_4+1/10 LD_{50} nBE-AF showed a significant improvement in hepatocyte morphology, as represented by the normal central vein (Figure 5D). Moreover, Kupffer cells were noticed around the portal tract, in addition to some congested blood vessels and a reduction in the size of the hepatic portal vein to a normal shape (Figure 5E). The livers of rats in the DEN+CCl_4+1/20LD_{50} nBE-AF group revealed moderate improvements in hepatocyte morphology, reductions in inflammation and degenerative changes, and reactive hepatocytes with condensed chromatin and small nuclei (Figure 5F).

Table 1: Oligonucleotide sequences used for real-time PCR analysis of the TNF-α and β-actin genes

Gene	Primer sequences	GenBank accession number
TNF-α	F: 5'-CCAGGAGAAAGTCAGCCTCCT -3' R: 5'-TCATACCAGGGCTTGAGCTCA -3'	NM_012675
ß-actin	F:5'-AAGTCCCTCACCCTCCCAAAAG -3' R: 5'-AAGCAATGCTGTCACCTTCCC -3'	V01217

Table 2: Determination of the LD_{50} of nBE-A

Group	Difference between consecutive doses (a)	No. of dead animals	Mean mortality between two consecutive doses (b)	a × b
Control	0	0	0	0
500 mg/kg b.wt.	500	0	0	0
1000 mg/kg b.wt.	500	0	0	0
1500 mg/kg b.wt.	500	0	0	0
2000 mg/kg b.wt.	500	0	0	0
2500 mg/kg b.wt.	500	0	0	0
3000 mg/kg b.wt.	500	0	0	0
3500 mg/kg b.wt.	500	0	0	0
4000 mg/kg b.wt.	500	0	0	0
4500 mg/kg b.wt.	500	2	1	500
5000 mg/kg b.wt.	500	3	2.5	1250
5500 mg/kg b.wt.	500	4	3.5	1750
6000 mg/kg b.wt.	500	5	4.5	2250
6500 mg/kg b.wt.	500	6	5.5	2750
Sum				8500

LD_{50} = LD - Σ (a × b)/N

LD is the lowest lethal dose among all animals in each group; N is the number of animals in each group; ∑ = the sum of (a × b).

LD_{50} =6500-8500/6= 6500-1416.6= 5083 mg/kg b.wt.

Table 3: Effect of nBE-AF on the serum levels of liver function markers in DEN-treated rats (Mean ± SE, n = 10)

Groups	ALT (U/L)	AST(U/L)	ALP(U/L)	Albumin(mg/dL)	Total protein(mg/dL)	TBL (mg/dL)
Control	67.74 ± 3.13[a]	169.42 ± 2.24[a]	131.60 ± 2.37[a]	3.98 ± 0.08[a]	7.56 ± 0.07[a]	0.70 ± 0.03[d]
DEN+CCl_4	118.36 ±2.97[d]	279.38±2.93[d]	197.00 ± 2.02[d]	2.24 ± 0.079[d]	4.25 ± 0.16[d]	1.19 ± 0.024[a]
DEN+CCl_4+1/10 LD_{50} nBE-AF	86.34 ± 1.08[b]	188.40±4.34[b]	156.40 ± 3.55[b]	3.38 ± 0.09[b]	6.6 ± 0.27[b]	0.76 ± 0.026[c]
DEN+CCl_4+1/20 LD_{50} nBE-AF	97.76 ± 2.20[c]	226.48±4.76[c]	180.00 ± 3.22[c]	2.98±0.05[c]	5.75 ± 0.07[c]	0.88 ± 0.019[b]
1/10 LD_{50} nBE-AF	70.26 ± 2.10[a]	174.38±0.82[a]	128.80 ± 2.63[a]	3.82 ± 0.14[a]	7.43± 0.15[a]	0.65 ± 0.02[d]
1/20 LD_{50} nBE-AF	69.32 ± 4.27[a]	174.40 ± 1.25[a]	130.20 ± 2.59[a]	3.92 ± 0.07[a]	7.13 ± 0.05[a]	0.67 ± 0.02[d]

Means within the same column carrying different superscripts are significantly different ($p < 0.05$).

Table 4: Effect of nBE-AF on oxidative stress markers in the liver of DEN-treated rats (Mean ± SE, n = 10)

Groups	SOD (U/g tissue)	CAT(U/g tissue)	GPx (ng/g tissue)	GSH(mmol/g tissue)	MDA(nmol/g tissue)
Control	11.00 ± 0.55[a]	66.00 ± 3.09[a]	0.74 ± 0.03[a]	1.19 ± 0.04[a]	82.53 ±1.53[d]
DEN+CCl_4	4.81± 0.71[d]	31.52 ± 2.06[d]	0.1 ± 0.014[d]	0.42 ± 0.03[d]	178.85 ± 1.68[a]
DEN+CCl_4+1/10 LD_{50} nBE-AF	8.73 ± 0.31[b]	54.00 ± 2.03[b]	0.62 ± 0.01[b]	0.92 ± 0.03[b]	98.19 ± 1.15[c]
DEN+CCl_4+1/20 LD_{50} nBE-AF	7.17 ± 0.09[a]	41.36 ±1.77[c]	0.44 ± 0.01[c]	0.75 ± o.02[c]	127.35 ± 1.49[b]
1/10 LD_{50} nBE-AF	11.25 ± 0.148[a]	66.40 ±2.86[a]	0.79 ± 0.01[a]	1.05 ± o.05[a]	82.96 ± 0.75[d]
1/20 LD_{50} nBE-AF	11.70 ± 0.51[a]	67.04 ± 1.77[a]	0.79 ± 0.01[a]	1.14 ± o.04[a]	81.16 ± 0.67[d]

Means within the same column carrying different superscripts are significantly different ($p < 0.05$).

Immunohistochemical findings

Immunohistochemical staining with the pro-apoptotic Bax antibody in rat liver tissue revealed weak expression in control and nBE-AF-treated rats (Figure 6A-C). The livers of rats in the DEN+CCl_4-treated group showed preneoplastic nodules with a marked reduction in the expression of Bax (Figure 6D). However, the livers of rats in the DEN+CCl_4+1/10 LD_{50} nBE-AF and DEN+CCl_4+1/20 LD_{50} nBE-AF groups showed increased nuclear and cytoplasmic expression of Bax (Figure 6E and F).

Immunohistochemical staining with the anti-apoptotic Bcl-2 protein in rat liver showed weak expression in control and nBE-AF-treated rats (Figure 7A-C). The livers of rats in the DEN+CCl_4-treated group exhibited preneoplastic nodules with marked expression of Bcl-2 (Figure7D), while the livers of rats in the groups treated with DEN+CCl_4+1/10 LD_{50} nBE-AF and DEN+CCl_4+1/20 LD_{50} nBE-AF showed moderate expression of Bcl-2 (Figure 7E and F).

nBE-AF Cytotoxicity

Conc µg/ml	HepG2 cells - 32 A
0.000	1.000000
5.000	0.737376
12.500	0.726812
25.000	0.308240
50.000	0.313170

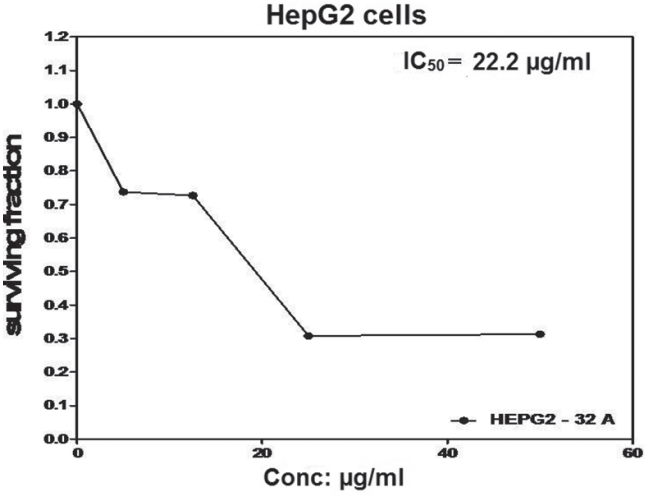

Figure 1: Cytotoxicity of nBE-AF against HepG2 cells

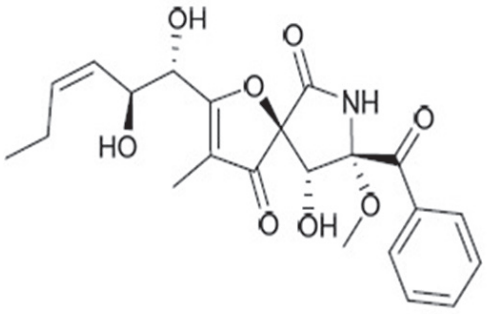

Figure 2: Chemical structure of pseurotin A isolated from nBE-AF

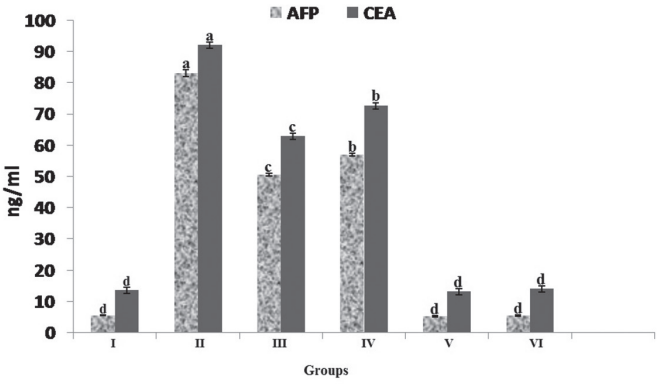

Figure 3: Effect of nBE-AF on the serum AFP and CEA levels in DEN-treated rats. The bars with differing letters indicate significant differences ($p<0.05$) (mean ±SE, n=10)

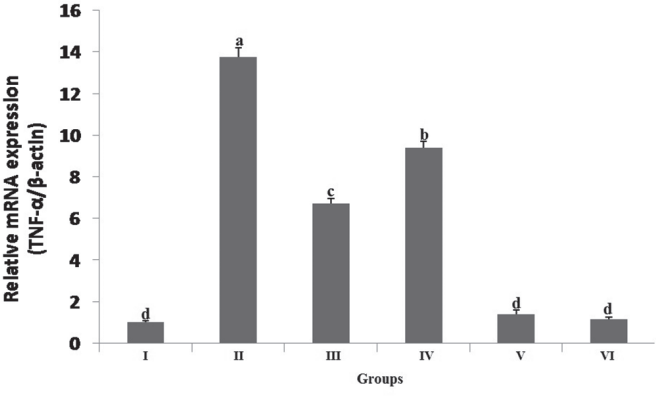

Figure 4: Relative expression levels of the TNF-α gene in the livers of control and experimental rats. The bars with differing letters indicate significant differences ($p < 0.05$) (mean ± SE, n=10)

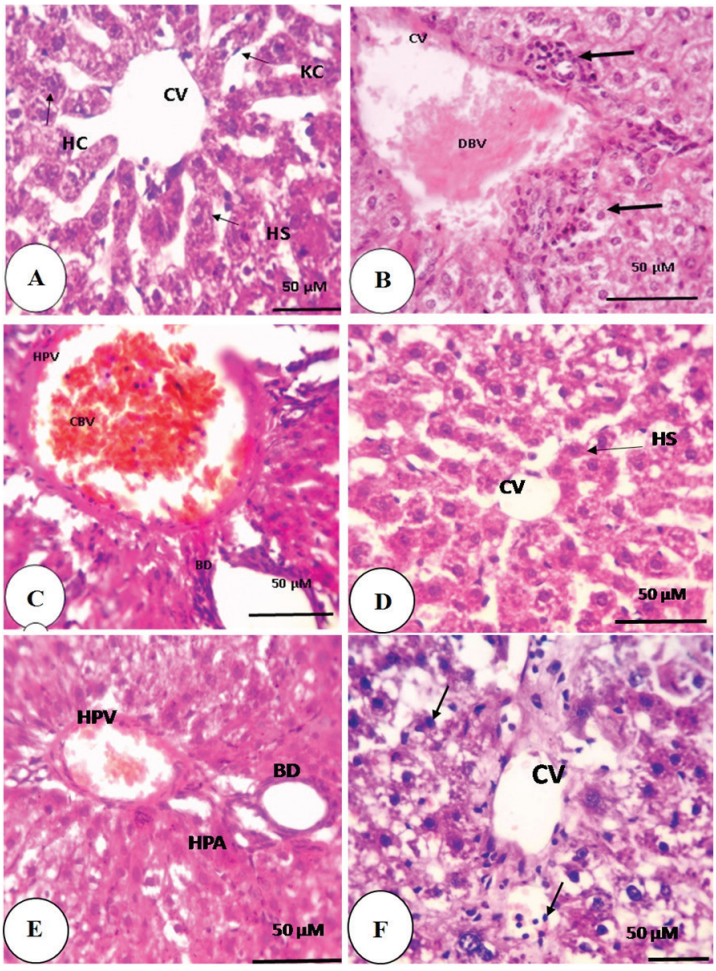

Figure 5: Photomicrographs of H&E-stained liver sections from rats in the control and experimental groups under light microscopy. A; The control group and the groups treated with nBE-AF alone at 1/10 and 1/20 LD_{50} showing normal architecture, indicating the nontoxic nature of nBE-AF. B, C; DEN+CCl_4-treated group showing the following abnormalities: B, Highly demarcated HCC near the central vein (CV) (thick arrow); some hepatocytes have vacuolated cytoplasm with deeply stained pyknotic nuclei. Dilated blood vessels (DBV) can also be seen; and C, Severe congested blood vessels (CBV) and hepatic portal vein (HPV), with portal vein dilation. D, E; DEN+CCl_4+1/10 LD_{50} nBE-AF-treated group showing considerable improvements in hepatocyte morphology. D; Normal central vein. E; The size of the hepatic portal vein was reduced to a normal shape, and Kupffer cells (KC) were visible around the portal tract, along with some congested blood vessels. F; DEN+CCl_4+1/20 LD_{50} nBE-AF-treated group showing moderate improvements in hepatocyte morphology, reductions in inflammation and degenerative changes, and reactive hepatocytes with condensed chromatin (arrowhead) and small nuclei. (HC: Hepatic cells, HS: Hepatic cells arranged in strands, HPA: Hepatic portal artery, BD: Bile duct)

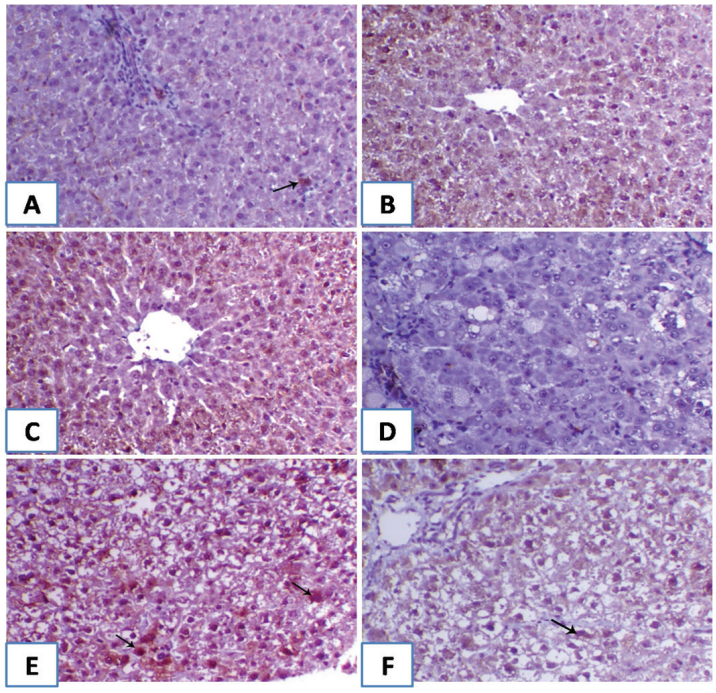

Figure 6: Immunohistochemical staining with Bax in liver tissue from rats in the control (A), 1/10 LD_{50} nBE-AF alone (B), 1/20 LD_{50} nBE-AF alone (C), DEN+CCl_4-treated (D), DEN+CCl_4+1/10 LD_{50} nBE-AF-treated (E) and DEN+CCl_4+1/20 LD_{50} nBE-AF-treated (F) groups. A-C; Weak expression of Bax (arrows). D; Preneoplastic nodule with a marked reduction in Bax expression. E, F; Increased nuclear and cytoplasmic expression of Bax (arrows) (200×)

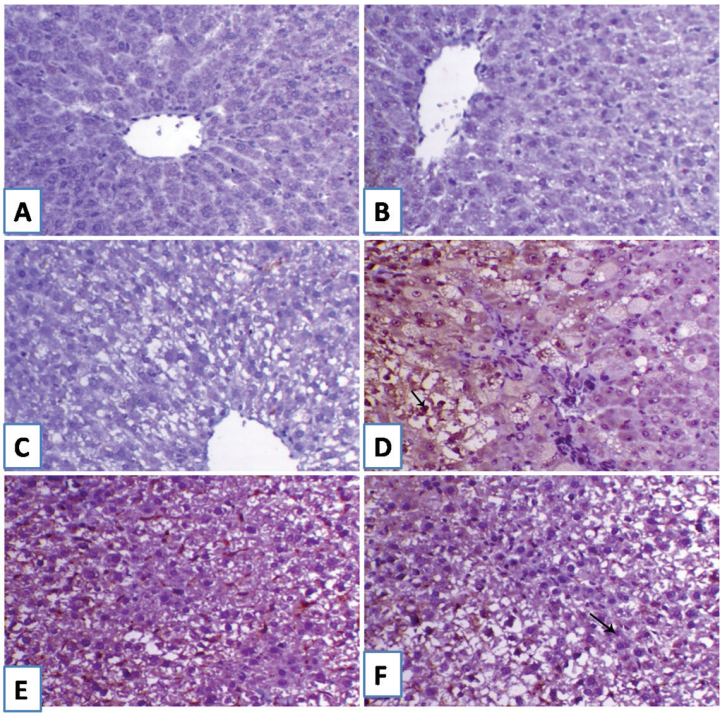

Figure 7: Immunohistochemical staining with Bcl-2 in liver tissue from rats in the control (A), 1/10 LD_{50} nBE-AF alone (B), 1/20 LD_{50} nBE-AF alone (C), DEN+CCl_4-treated (D), DEN+CCl_4+1/10 LD_{50} nBE-AF-treated (E) and DEN+CCl_4+1/20 LD_{50} nBE-AF-treated (F) groups. A-C; Weak expression of Bcl-2. D; Preneoplastic nodule with marked expression of Bcl-2(arrows). E, F; Moderate expression of Bcl-2 (arrows) (200×)

Discussion

In recent years, interest in the use of bioactive metabolites of microorganisms such as actinomycetes and fungi as possible chemopreventive and chemotherapeutic agents against HCC has been increasing worldwide. These derived compounds inhibited the growth and proliferation of tumour cells (31).This study investigated the *in vitro* anticancer activity of nBE-AF on HepG2 cells as well as its chemopreventive potential against DEN+CCl_4-induced HCC in rats. Our results showed that nBE-AF has significant cytotoxicity towards HepG2 cells, with an IC_{50} of 22.2 µg/ml. Therefore, we suggest that nBE-AF has strong cytotoxic activity according to the guidelines of The American National Cancer Institute, which describe an extract with strong cytotoxic activity as an anticancer agent if its IC_{50} value is less than 30 mg/ml (32). In the present study, the major compound isolated from nBE-AF was identified as pseurotin A. Four pseurotin analogues were reported to exhibit potent cytotoxicity against the human breast cancer cell line MCF-7, with the more active pseurotin D inhibiting MCF-7 cell growth with an IC_{50} value of 15.6 µM (33).

DEN and CCl_4 induced liver damage in rats, as indicated by significant increases ($p < 0.05$) in the serum transaminase (ALT and AST), ALP and TBL levels relative to those in control group. Elevations in transaminase levels are considered the most sensitive markers for diagnosing hepatocellular damage (34).The elevated serum ALT and AST levels in DEN + CCl_4-treated rats may be attributed to DEN-induced hepatic damage associated with the loss of the functional integrity of the cell membrane and the leakage of cellular enzymes from neoplastic cells into the circulation (35). Moreover, the elevated ALP activity reflected pathological alterations in biliary flow, and the increased TBL level indicated a non-specific alteration in plasma membrane integrity and permeability (6). Serum protein levels can also be used as a marker of liver function. Administration of DEN and CCl_4 caused a significant reduction in the serum albumin and total protein levels, indicating hepatocellular dysfunction. The DEN + CCl_4-induced liver damage observed in the present study was consistent with that seen in previous studies (6, 31). Our results showed that DEN and CCl_4 elicited a significant increase ($p < 0.05$) in the levels of serum tumour markers (AFP and CEA) relative to those levels in the control group. These findings coincided with those in previous studies showing increased levels of serum tumour markers,

including AFP and CEA, following treatment with DEN and CCl_4 in rats (6, 36). AFP is an oncofoetal serum glycoprotein that is normally produced by immature liver cells in the foetus but is gradually lost during development, becoming almost absent in healthy adults (37), and is an excellent marker for diagnosing HCC (38). CEA is a 180–200 kDa, heavily glycosylated protein belonging to the immunoglobulin supergene family. CEA is commonly detected at a high level in the serum of patients with liver malignancy (39). Additionally, the CEA level is elevated in the serum of patients with various other cancers, such as lung, colon, ovarian and breast cancers (40). Furthermore, administration of DEN and CCl_4 caused hepatic oxidative damage in rats, as evidenced by the reductions in antioxidant enzyme (SOD, CAT and GPx) activity and the GSH concentration, along with increased lipid peroxidation (MDA) in the livers of rats in the DEN + CCl_4-treated group relative to these parameters in control group. These results were consistent with those in previous reports (6, 36, 41). Administration of DEN has been reported to generate products of lipid peroxidation such as 4-hydroxynonenal and MDA that may interact with different molecules, resulting in oxidative stress and carcinogenesis (42). Additionally, DEN-induced oxidative stress may be due to the generation of ROS during the metabolic biotransformation of DEN (43). Oxidative stress results in carcinogenesis by several mechanisms involving damage to lipids, proteins and DNA; alterations in intracellular signalling pathways; and changes in gene expression—these events, in turn, promote abnormal cell growth and carcinogenesis (44). We observed significant ($p < 0.05$) upregulation of TNF-*a* gene expression in the livers of DEN+CCl_4-treated rats relative to that in control group. Similarly, hepatic TNF-*a* gene expression was significantly increased in DEN-treated mice (45, 46). TNF-*a* is a pro-inflammatory cytokine involved in cancer owing to its ability to activate the oncogenic transcription factors nuclear factor kappa B (NF-κB) and activator protein 1 (AP-1) in epithelial cells, leading to the promotion of cell proliferation and survival. Consequently, NF-κB activation plays a vital role in tumour cell growth and invasion (47, 48). In addition, TNF-*a* acts as a growth factor in the majority of tumour cells and can affect all stages of tumour development, including initiation, promotion and metastasis (49, 50). Interestingly, co-treatment with nBE-AF ameliorated DEN+CCl_4-induced hepatic damage by significantly ($p < 0.05$) restoring the levels of liver function markers in a dose-dependent manner. Therefore, our results indicate that nBE-AF facilitates parenchymal cell regeneration in the liver, thus protecting membrane integrity by reducing enzyme leakage induced by the carcinogenic effects of DEN and CCl_4. These findings were in accordance with those of a previous study showing that the alkaloid berberine ameliorated liver damage induced by CCl_4 in rats (51). Concomitant treatment with nBE-AF and DEN+CCl_4 significantly ($p < 0.05$) decreased the levels of serum tumour markers, including AFP and CEA, relative to those in the DEN+CCl_4-treated group. This finding suggested that nBE-AF reduced the tumour incidence rate. This hypothesis was supported by the pro-apoptotic effect of nBE-AF observed in the present study, as evidenced by the increased immunohistochemical expression of Bax and decreased expression of Bcl-2 in the livers of rats in the groups co-treated with nBE-AF (III and IV). Interestingly, administration of nBE-AF mitigated DEN+CCl_4-induced hepatic oxidative damage by restoring the activity of antioxidant enzymes (SOD, CAT and GPx) and the levels of GSH and MDA towards the control values. This effect may be due to the antioxidant and free radical scavenging activities of pseurotin A, the major secondary metabolite isolated from nBE-AF (52). In a similar study, the alkaloid canadine showed antioxidant activity against oxidative stress induced by tert-butylhydroperoxide in rat hepatocytes (53). Notably, significant ($p < 0.05$) dose-dependent downregulation of TNF-α gene expression was observed in the livers of rats in the groups co-treated with nBE-AF(III and IV) relative to that in rats in the DEN+CCl_4-treated group. Similarly, the alkaloid crebanine inhibited TNF-α-induced NF-κB activation in A549 human lung adenocarcinoma cells. Additionally, crebanine suppressed the TNF-α-mediated expression of proteins implicated in cancer cell invasion, such as matrix metalloproteinase 9 (54). Our findings demonstrated that nBE-AF exerts anti-inflammatory and anticancer effects through the downregulation of hepatic TNF-α gene expression, which plays an essential role in tumour development and metastasis via NF-κB activation. Regarding the immunohistochemical expression of the pro-apoptotic Bax and anti-apoptotic Bcl-

2 proteins in the liver, these proteins are key factors that regulate apoptosis and determine cell death or survival (55). The present results showed preneoplastic nodules with a marked reduction in Bax expression in the DEN+CCl4-treated rats. However, rats in the groups co-treated with nBE-AF (III and IV) exhibited increased nuclear and cytoplasmic expression of Bax. The anti-apoptotic protein Bcl-2 is implicated in cancer initiation and progression by promoting the survival of transformed cells. Therefore, Bcl-2 is the main target for innovative specific anticancer therapeutics. In addition, the present results showed that administration of DEN and CCl_4 caused a marked increase in the expression of Bcl-2 relative to that in the control group. Consistent with our results, other studies have indicated that Bcl-2 is overexpressed in various types of cancers (56). In contrast, the groups co-treated with nBE-AF exhibited a marked reduction in Bcl-2 expression relative to that in the DEN+CCl_4-treated group. These findings were consistent with those in a similar study showing that 6-methoxydihydrosanguinarine induced apoptosis in HepG2 cells via upregulation of Bax and downregulation of Bcl-2 (57).The current findings confirmed that nBE-AF could induce apoptosis in HCC cells and eventually inhibit tumour cell proliferation in rats with DEN+CCl_4-induced HCC.

The antioxidant, anti-proliferative and anticancer activities exhibited by nBE-AF may contribute to its chemopreventive effect against DEN+CCl_4-induced hepatocarcinogenesis in rats (13, 58).

Our aforementioned data were corroborated by the liver histopathological findings. Histopathological examination of the livers of DEN+CCl_4-treated rats revealed marked architectural changes, with highly demarcated HCC near the central vein. These findings were consistent with those of previous reports (6, 36).

Co-administration of a 1/10 LD_{50} dose of nBE-AF significantly ameliorated these pathological lesions. However, co-treatment with a 1/20 LD_{50} dose of nBE-AF produced moderate improvements in hepatocyte morphology and reduced inflammation and degenerative changes. Our results were consistent with those of similar studies showing that the alkaloid berberine exerted hepatoprotective effects against histological damage induced by CCl_4 in rats (59) and by doxorubicin in mice (60).

Conclusion

The results of this study demonstrated that nBE-AF exhibited anticancer activity on HepG2 cells *in vitro* and exerted a dose-dependent beneficial protective effect against DEN+CCl_4-induced hepatocarcinogenesis in rats by restoring the serum levels of tumour and hepatic function markers, enhancing the liver antioxidant status, downregulating the hepatic TNF-*a* gene expression and minimizing histological alterations in the liver. In addition, nBE-AF inhibited HCC cell proliferation through the induction of apoptosis via increased Bax expression and decreased Bcl-2 expression. The anti-carcinogenic effect of pseurotin A isolated from *A. Fumigatus* could be attributed to its antioxidant, anti-inflammatory, cytotoxic and pro-apoptotic activities. Therefore, nBE-AF could be a candidate chemopreventive agent for hepatic cancer.

Acknowledgements

We would like to thank Dr. Fathy El-Shaer Mohammed, Lecturer of Comparative Anatomy, Zoology Department, Faculty of Science, Al-Azhar University, Cairo, Egypt for his guidance and support for the histopathological findings.

References

1. WHO. World cancer day. Geneva : World Health Organization, 2013. [Online] http://www.who.int/cancer/en/index.htmL

2. Chatterjee R, Mitra A. An overview of effective therapies and recent advances in biomarkers for chronic liver diseases and associated liver cancer. Int Immunopharmacol 2015; 24: 335–45.

3. Farazi PA, DePinho RA. Hepatocellular carcinoma pathogenesis: from genes to environment. Nat Rev Cancer 2006; 6: 674–87.

4. Sivaramakrishnan V, Shilpa PN, Praveen Kumar VR, Niranjali Devaraj S. Attenuation of N-nitrosodiethylamine-induced hepatocellular carcinogenesis by a novel flavonol-Morin. Chem Biol Interact 2008; 171: 79–88.

5. Subramanian P, Mirunalini S, Dakshayani KB, Pandi-Perumal SR, Trakht I, Cardinali DP. Prevention by melatonin of hepatocarcinogenesis in rats injected with N-nitrosodiethylamine. J Pineal Res 2007; 43: 305–12.

6. Singh BN, Singh BR, Sarma BK., Singh HB. Potential chemoprevention of N-nitrosodiethylamine-induced hepatocarcinogenesis by polyphenolics from *Acacia nilotica* bark. Chem Biol Interact 2009; 181: 20–8.

7. Sadik NA, EL-Maraghy SA, Ismail MF. Diethylnitrosamine-induced hepatocarcinogenesis in rats: possible chemoprevention by blueberries. Afr J Biochem Res 2008; 2: 81–7.

8. Thoppil RJ, Bhatia D, Barnes KF, et al. Black currant anthocyanins abrogate oxidative stress through Nrf2- mediated antioxidant mechanisms in a rat model of hepatocellular carcinoma. Curr Cancer Drug Targets 2012; 12: 1244–57.

9. Sporn MB, Suh N. Chemoprevention: an essential approach to controlling cancer. Nat Rev Cancer 2002; 2: 537–43.

10. Aggarwal BB, Shishodia S. Molecular targets of dietary agents for prevention and therapy of cancer. Biochem Pharmacol 2006; 71: 1397–421.

11. Du L, Li D, Zhu T, et al. New alkaloids and diterpenes from a deep ocean sediment derived fungus *Penicillium* sp. Tetrahedron 2009; 65: 1033–9.

12. Fujiki H, Mori M, Nakayasu M, Terada M, Sugimura T, Moore RE. Indole alkaloids: dihydroteleocidin B, teleocidin, and lyngbyatoxin A as members of a new class of tumor promoters. Proc Natl Acad Sci USA 1981; 78: 3872–6.

13. Ge HM, Yu ZG, Zhang J, Wu JH, Tan RX. Bioactive alkaloids from endophytic *Aspergillus fumigatus*. J Nat Prod 2009; 72: 753–5.

14. Bloch P, Tamm C, Bollinger P, Petcher T J, Weber HP. Pseurotin, a new metabolite of *Pseudeurotium ovalis* stolk having an unusual hetero-spirocyclic system. (Preliminary communication). Helv Chim Acta 1976; 59: 133–7.

15. Liu R, Gu Q, Zhu W, et al. 10-Phenyl-[12]-cytochalasins Z7, Z8, and Z9 from the marine-derived fungus *Spicaria elegans*. J Nat Prod 2006; 69: 871–5.

16. Skehan P, Storeng R, Scudiero D, et al. New colorimetric cytotoxicity assay for anticancer-drug screening. J Natl Cancer Inst 1990; 82: 1107–12.

17. Turner R. Quantal responses. Calculation of ED50. In: Turner RA, Hebborn P, eds. Screening methods in pharmacology. 1st ed. New York : Academic Press, 1965: 61–3.

18. Sarkar A, Basak R, Bishayee A, Basak J, Chatterjee M. Beta-carotene inhibits rat liver chromosomal aberrations and DNA chain break after a single injection of diethylnitrosamine. Br J Cancer 1997; 76: 855–61.

19. Bergmeyer HU, Scheibe P, Wahlefeld AW. Optimization of methods for aspartate aminotransferase and alanine aminotransferase. Clin Chem 1978; 24: 58–73.

20. King EJ, Armstrong AR. 1988. Calcium, phosphorus and phosphatases, In: Varley H, eds. Practical clinical biochemistry. New Delhi, India : CBS Publishers, 1988: 458.

21. Grant GH, Silverman LM, Christenson RH. Amino acids and proteins. In: Tietz NW, eds. Fundamentals of clinical chemistry. 3rd ed. Philadelphia : WB Saunders, 1987: 291–345.

22. Tietz NW. Fundamentals of clinical chemistry. 2nd ed. Madison : Wisconsin University, 1976.

23. Tietz NW. Clinical guide to laboratory tests. 3rd ed. Philadelphia : W.B. Saunders, 1995.

24. Nishikimi M, Roa NA, Yogi K. The occurrence of superoxide anion in the reaction of reduced phenazinemethosulphate and molecular oxygen. Biochem Bioph Res Common 1972; 46: 849–54.

25. Aebi H. Catalase invitro. Methods Enzymol 1984; 105: 121–26.

26. Gross RT, Bracci R, Rudolph N, Schroeder E, Kochen JA. Hydrogen peroxide toxicity and detoxification in the erythrocytes of newborn infants. Blood 1967; 29: 481–93.

27. Beutler E, Duron O, Kelly BM. Improved method for the determination of blood glutathione. J Lab Clin Med 1963; 61: 882–8.

28. Ohkawa H, Ohishi N, Yagi K. Assay for lipid peroxides in animal tissues by thiobarbituric acid reaction. Anal Biochem 1979; 95: 351–8.

29. Bancroft JD, Gamble M. Theory and practice of histological techniques. 6th ed. London : Churchill Livingstone ; London ; New York : Philadelphia /Elsevier, 2008.

30. Shi SR, Key ME, Kalra KL. Antigen retrieval in formalin-fixed, paraffin-embedded tissues: an enhancement method for immunohistochemical staining based on microwave oven heating of tissue sections. J Histochem Cytochem 1991; 39: 741–8.

31. Pereira DM, Cheel J, Areche C, et al. Anti-proliferative activity of meroditerpenoids isolated from the brown alga *Stypopodium flabelliforme* against several cancer cell lines. Mar Drugs 2011; 9: 852–62.

32. Itharat A, Ooraikul B. Research on Thai medicinal plants for cancer treatment. Med Plant

Res 2007; 1: 287–317.

33. Thohinung S, Kanokmedhakul S, Kanokmedhakul K, Kukongviriyapan V, Tusskorn O, Soytong K. Cytotoxic 10-(indol-3-yl)-[13]cytochalasans from the fungus *Chaetomium elatum* ChE01. Arch Pharm Res 2010; 33: 1135–41.

34. Plaa GL, Hewitt WR. Detection and evaluation of chemically induced liver injury. In: Wallace Hayes A, eds. Principles and methods of toxicology. New York : Raven Press, 1989: 399–628.

35. Dakshayani KB, Subramanian P, Manivasagam T, Essa MM, Manoharan S. Melatonin modulates the oxidant-antioxidant imbalance during N-nitrosodiethylamine induced hepatocarcinogenesis in rats. J Pharm Pharm Sci 2005; 8: 316–21.

36. Hussain T, Siddiqui HH, Fareed S, Vijayakumar M, Rao CV. Evaluation of chemopreventive effect of *Fumaria indica* against N-nitrosodiethylamine and CCl4-induced hepatocellular carcinoma in Wistar rats. Asian Pac J Trop Biomed 2012; 5: 623–9.

37. Sell S, Becker F, Leffert H, et al. Alphafetoprotein as a marker for early events and carcinoma development during chemical hepatocarcinogenesis. In: Milman HA, Sell S, eds. Application of biological markers to carcinogen testing. Boston : Springer, 1983: 271–93. (Environ Sci Res 1983; volume 29.)

38. 38. Liu C, Xiao GQ, Yan LN, et al. Value of α-fetoprotein in association with clinicopathological features of hepatocellular carcinoma. World J Gastroenterol 2013; 19: 1811–9.

39. Maeda M, Tozuka S, Kanayama M, Uchida T. Hepatocellular carcinoma producing carcinoembryonic antigen. Dig Dis Sci 1988; 33: 1629–31.

40. Zamcheck N, Steele GD, Thomas P, Meyer RJ. Use of carcinoembryonic antigen in the monitoring of patients. In: Rose NR, Friedman H Fahey JL, eds. The manual of clinical immunology. Washington : American Society for Microbiology, 1986: 802–9.

41. Hussein RH, Khalifa FK. The protective role of ellagitannins flavonoids pretreatment against N-nitrosodiethylamine induced-hepatocellular carcinoma. Saudi J Biol Sci 2014; 21: 589–96.

42. Hietanen E, Ahotupa M, Bartsch H. Lipid peroxidation and chemically induced cancer in rats fed lipid rich diet. In: Lapis K, eds. Carcinogenesis and tumor progression. Budapest : Akademiai Kiado,1987: 9–16.

43. Harman D. Free radical theory of aging: origin of life, evolution, and aging. Age 1980; 3: 100–2.

44. Klaunig JE, Kamendulis LM. The role of oxidative stress in carcinogenesis. Annu Rev Pharmacol Toxicol 2004; 44: 239–67.

45. Shimizu M, Yasuda Y, Sakai H, et al. Pitavastatin suppresses diethylnitrosamine-induced liver preneoplasms in male C57BL/KsJ-db/dbobese mice. BMC Cancer 2011; 11: 281.

46. Yang Y, Guo Y, Tan S, Ke B, Tao J, Liu H, Wu B. Beta-Arrestin1 enhances hepatocellular carcinogenesis through inflammation-mediated Akt signalling. Nat Commun 2015; 6: 7369.

47. Matthews CP, Colburn NH, Young MR. AP-1 a target for cancer prevention. Curr Cancer Drug Targets 2007; 7: 317–24.

48. Balkwill F, Tumour necrosis factor and cancer. *Nat Rev Cancer* 2009; 9: 361–371.

49. Aggarwal BB, Gupta SC, Kim JH. Historical perspectives on tumor necrosis factor and its superfamily: 25 years later, a golden journey. Blood 2012; 119: 651–65.

50. Shanmugam MK, Sethi G. 2013. Role of epigenetics in inflammation-associated diseases. In: Kundu T, eds. Epigenetics: development and disease. Dordrecht : Springer, 2013: 627–57. (Subcell Biochem, volume 61)

51. Feng Y, Siu KY, Ye X, et al. Hepatoprotective effects of berberine on carbon tetrachloride-induced acute hepatotoxicity in rats. Chin Med 2010; 5: 33.

52. Lu QQ, Tian JM, Wei J, Gao JM. Bioactive metabolites from the mycelia of the basidiomycete *Hericium erinaceum*. Nat Prod Res 2014; 28: 1288–92.

53. Correché ER, Andujar SA, Kurdelas RR, Lechón MJG, Freile ML, Enriz RD. Antioxidant and cytotoxic activities of canadine: Biological effects and structural aspects. Bioorg Med Chem 2008; 16: 3641–51.

54. Yodkeeree S, Pompimon W, Limtrakul P. Crebanine, an aporphine alkaloid, sensitizes TNF-alpha-induced apoptosis and suppressed invasion of human lung adenocarcinoma cells A549 by blocking NF-kappaB-regulated gene products. Tumour Biol 2014; 35: 8615–24.

55. Korsmeyer SJ. BCL-2 gene family and the regulation of programmed cell death. Cancer Res 1999; 59 (7 Suppl): 1693s–700.

56. Akl H, Vervloessem T, Kiviluoto S, et al. A dual role for the anti-apoptotic Bcl-2 protein in cancer: mitochondria versus endoplasmic reticu-

lum. BBA Mol Cell Res 2014; 1843: 2240–52.

57. Yin HQ, Kim YH, Moon CK, Lee BH. Reactive oxygen species-mediated induction of apoptosis by a plant alkaloid 6-methoxydihydrosanguinarine in HepG2 cells. Biochem Pharmacol 2005; 70: 242–8.

58. Martínez-Luis S, Cherigo L, Arnold E, Spadafora C, Gerwick W, Cubilla-Rios L. Antiparasitic and anticancer constituents of the endophytic fungus *Aspergillus* sp. strain F1544. Nat Prod Commun 2012; 7: 165–8.

59. Feng Y, Siu K.-Y, Ye X, Wang N, Yuen MF, Leung CH, Kobayashi S. Hepatoprotective effects of berberine on carbon tetrachloride-induced acute hepatotoxicity in rats. Chin Med 2010; 5: 33.

60. Zhao X, Zhang J, Tong N, Chen Y, Luo Y. Protective effects of berberine on doxorubicin-induced hepatotoxicity in mice. Biol Pharm Bull 2012; 35: 796–800.

PSEUROTIN A IZ GLIVE *Aspergillus fumigatus* Fr. AUMC 8002 ZAVIRA RAST KARCINOMA JETER *IN VITRO* IN *IN VIVO*

G. A. Helal, F. A. Ahmed, A. Askora, T. M. Saber, S. M. Rady

Povzetek: V študiji so raziskali *in vitro* in *in vivo* protirakasto aktivnost pseurotina A, pridobljenega iz n-butanolnega izvlečka glive *Aspergillus fumigatus* Fr. AUMC 8002 (nBE-AF), na karcinom jeter. *In vitro* protirakasta aktivnost nBE-AF je bila spremljana pri humani celični liniji jetrnega karcinoma (HepG2) z uporabo analize sulforhodamin-B (SRB). Pri podganah so intraperitonealno določili povprečni smrtni odmerek (LD_{50}) nBE-AF. Jetrni karcinom je bil pri podganah sprožen z enkratno intraperitonealno injekcijo dietilnitrozamina (DEN) (200 mg/kg telesne teže), čemur so sledile podkožne injekcije ogljikovega tetraklorida (CCl_4) (3 ml/kg) enkrat tedensko 6 tednov. Po dodajanju teh rakotvornih snovi so 1/10 in 1/20 odmerka LD_{50} nBE-AF aplicirali vsak dan intraperitonealno. NBE-AF je pokazal pomembno citotoksično aktivnost proti celicam HepG2. Uporaba DEN in CCl4 je značilno povečala serumske vrednosti jetrnih funkcij in tumorskih markerjev ter znatno zmanjšala izražanje gena za faktor tumorske nekroze α (TNF- α). Poleg tega sta DEN in CCl_4 zmanjšala imunohistokemično izražanje gena Bax in povečala izražanje gena Bcl-2 v jetrih. Sočasno zdravljenje z nBE-AF je zmanjšalo z DEN + CCl_4 sprožene spremembe v jetrih v povezavi z velikostjo odmerka. Histopatološka ocena jeter je potrdila zgoraj navedene biokemične rezultate. Rezultati so potrdili, da je nBE-AF preko svojega glavnega izoliranega sekundarnega metabolita pseurotina A izkazal protirakasti učinek na jetra in bi se lahko v prihodnosti morda uporabljal kot zdravilo za zdravljenje karcinoma jeter.

Ključne besede: izvleček *Aspergillus fumigatus*; pseurotin A; karcinom jeter; protirakasto; citotoksično